FPGA-based Embedded Cyber-Physical Platform to Assess Gait and Postural Stability in Parkinson Disease

Published Source:
D. De Venuto, V. F. Annese, G. Mezzina and G. Defazio, "FPGA-Based Embedded Cyber-Physical Platform to Assess Gait and Postural Stability in Parkinson's Disease," in IEEE Transactions on Components, Packaging and Manufacturing Technology, vol. 8, no. 7, pp. 1167-1179, July 2018, doi: **10.1109/TCPMT.2018.2810103**.

FPGA-based Embedded Cyber-Physical Platform to Assess Gait and Postural Stability in Parkinson Disease

D. De Venuto, V.F. Annese, G. Mezzina, G. Defazio

***Abstract* - Abnormal gait and postural instability are common disorders in people affected by Parkinson's disease (PD). This paper proposes an embedded cyber-physical system for the identification and the real-time extraction of highly selective diagnostic indexes for PD patients. A non-invasive wearable and wireless architecture for both gait analysis and postural instability detection has been proposed and implemented on a programmable hardware. The combined analysis of EEG and EMG allows studying the motor cortex activity through the Movement Related Potentials (MRPs), determining a novel set of indexes that could be used for the PD diagnosis and classification. In a future perspective of an ASIC implementation, the real-time data processing has been fully realized on the Altera Cyclone V FPGA, without interactions with embedded processor architecture.**

Referring to an Altera Cyclone V SE 5CSEMA5F31C6N device, the whole implemented architecture exploits the 90% of the available FPGA ALMs, the 74% of the manageable registers and the 10.3% of the total memory, as well as the 29.7% wires utilization. Furthermore, the system is able to provide the outputs in about 57ms with a dynamically power dissipation of 89mW.

The platform has been tested in-vivo on 2 Parkinson's patients and 2 healthy subjects (control group) covering three typical diagnostic scenarios: PD vs. Controls, Drug Treatment Evaluation and Involuntary Movements detection.

***Index Terms* - Gait Analysis, EEG-EMG Coupling, Parkinson, Assistive Technology, Embedded Cyber-Physical System**

I. Introduction

One of the current challenges in brain-machine interfacing is to characterize and decode the limb kinematics from brain signals. Recent research work states that it is possible to do so based on low frequency electroencephalographic components. Several the applications in neurodegenerative diseases, as well as the Parkinson's diseases.

Parkinson's disease (PD) is one of the most common neurodegenerative diseases [1]. Although several motor and non-motor symptoms may occur over the course of the disease, the PD diagnosis is based on the detection of a few cardinal motor signs including bradykinesia, rest tremor, and rigidity in different body parts, gait impairment and postural instability. These motor features result, at least in part, from a selective and progressive loss of dopaminergic neurons in the substantia nigra pars compacta. Although symptomatic dopamine-replacement therapy is of benefit in the early stages of PD, it is also linked with the development of often disabling motor complications like the wearing-off phenomenon (which is linked to the end-of-dose deterioration) and abnormal involuntary movements (dyskinesia) [2, 3]. Several clinical rating scales have been proposed to stratify the disease. The Unified Parkinson's Disease Rating Scale (UPDRS) [4] is the most widely used scale in clinical practice and research to evaluate tremor, rigidity and bradykinesia in different body parts, as well as speech, facial expression, gait impairment and postural instability by 0 to 4 grading. Like other clinical scales, the UPDRS is based on clinical grounds rather than systematic quantification and, for this reason, it can be biased. This raises the need for objective methods ensuring greater precision in evaluating PD motor signs.

In this paper, we detail the implementation and testing a real-time FPGA-based wearable platform for PD stratification by synchronized cortico-muscular analysis. The programmable device exploits the synchronized study of electroencephalography (EEG) and electromyography (EMG), calculating in real-time, a set of indexes (postural instability, involuntary movements, pre-motor potentials, drug-related benefits) according to the UPDRS standard scale. The complete cyber-physical system has been implemented on an FPGA in order to achieve and hardware implementation which can guarantee a real-time operation even when large data needs to be processed. The platform has been tested in-vivo on 2 PD patients and 2 healthy subjects in 3 different real-life scenarios:

(1) PD stratification based on cortico-muscular analysis;
(2) Gait analysis to assess postural instability:
(3) Benefits evaluation of short-term levodopa treatments.

The structure of the paper is the following: Sec. 2 analyzes the

Manuscript submitted on September 29 2017

D. De Venuto and G. Mezzina are with the Department of Electrical and Information Engineering (DEI), Politecnico di Bari, Italy.

V.F. Annese is with h the Micro Systems Technology Group, Department of Electronics and Electrical Engineering, The University of Glasgow, Glasgow G12 8LT, U.K.

G. Defazio is with the Department of Basic Medical Sciences, Neuroscience and Sense Organs, "Aldo Moro" University of Bari, Italy.

current state of the art, briefly describes the basic medical knowledge, the architecture and the FPGA implementation; in Sec. 3, the experimental results are shown. Sec. 4 concludes the paper giving the perspective of the proposed cyber-physical system (CPS).

II. Methods

A. State of the Art

At the current state of the art, several tools aiming to stratify the severity of PD by smart sensors processing have been proposed [5]. These included video systems for gait monitoring [6], GPS approaches [7] or movement tracker systems [7 -10]. All the proposed beneficial tools have some drawbacks. The video system in [6] allows accurate investigation and provides useful information related to the gait analysis (e.g. bradykinesia, rest tremor, rigidity and postural instability), nevertheless, it is limited to an ambulatory application and needs extensive analysis. High accuracy satellite positioning [7] can monitor outdoor walking, but it returns only few walking parameters.

Ambulatory gait monitoring systems, using tiny and wearable motion sensors, can monitor the status of the disease anytime and anywhere. Among these systems, there are the eGaIT system [8], the Parkinson's Kinetigraph (PKG) based system [10] and the wearable activity monitoring system (W-AMS) developed in [11]. The eGaIT [8] approach reaches 91% of accuracy in severe PD recognition, but the accuracy goes down to 81% when the impairment level decreases. Although it is a good complementary tool for daily clinical workup, eGaIT does not provide useful information about bradykinesia and dyskinesia. The PKG [10] system is characterized by low encumbrance of the acquisition sensors and, also, it operates offline. The W-AMS [11] extracts visual characteristics and 3D position by inertial sensors. However, general gait characteristics are frequently missed in severe PD patients and sometimes there are noise peaks that could be confuse with gait signals [11]. Rodríguez-Martín et al. in [12] have realized a prototype of an inertial measurement unit performing both real-time analysis of Parkinson's disease symptoms during gait and fall detection. The proposed system may be applicable to the dyskinesia recognition or in defining the side effect in dopaminergic replacement treatments [13]. Despite the wide range of analyzed symptoms, as well as the classification capability [13], the data extracted need complex post processing to provide reliable diagnosis and this makes the domestic diagnosis not feasible. Also, noteworthy is the so-called "PERFORM" system proposed in [14]. The system includes four tri-axial accelerometers used to record the accelerations of the movements at each patient extremity, one accelerometer/gyroscope on the waist and an acquisition unit, wearable and constantly monitoring the PD patient's features (i.e. tremor, freezing, Levodopa inducted dyskinesia and bradykinesia). The overall extracted data provide a good description of the above-stated parameters, but the data handling needs post-processing and off-line classification [14]. All the above-mentioned works are surely remarkable, nevertheless, the complexity of the post-processing [6, 10, 11, 14] requires computational times and resources too demanding for real-time applications in a real-life scenario. Indeed, as shown in Table I, which compare our work at the current state of the art, the 50% of the analyzed solution uses dedicated software, installed on a computer. Two solutions adopt a micro-controller solution, but only in a single case, the limited computational effort allows the system to be used in a real time context.

Additionally, none of them provides information about the coupling between motor and cerebral activity. The lack of such information is critical.

In fact, the combined analysis of cortical and muscular signals allows better understanding the cerebral activity leading to movement under physiological and pathological conditions.

Although the combined evaluation of EEG and EMG signals is more significant for PD diagnosis [15-17], the requirement for computational resources becomes even more onerous.

In fact, while a 1s data stream from 1 accelerometer (11bit@50Hz) [8] requires only 550 bits, a 1s second data stream for 1 EEG channel (24bit @500Hz) and 1 EMG channel (16bit@500Hz) requires 20kb. In order to guarantee the real-time processing of such a large dataset, a dedicated processor – ideally an Application-Specific Integrated Circuit (ASIC) – and an optimized strategy for data compression are needed. In this work, we have therefore implemented our system on an Altera Cyclone V SE 5CSEMA5F31C6N device in order to demonstrate that an ASIC for PD stratification processing EEG and EMG data in real-time can be implemented.

TABLE I. CURRENT STATE OF THE ART

	Aim	Sensors & Processing unit	Wearable	RT	RL-S	Brain signal
[6]	GA	Camera, n.d.	×	×	×	×
[7]	GA	GPS, Computer	✓	✓	×	×
[8]	PDS	Acc + gyro, Computer	✓	✓	✓	×
[9]	PDS	Acc, Computer	✓	×	✓	×
[10]	PDS	Acc + FS, Computer	✓	×	✓	×
[11]	PDS	Inertial unit, n.d.	✓	×	✓	×
[12]	PDS	Inertial unit, Microcontroller	✓	✓	×	×
[14]	PDS	Acc + gyro, Microcontroller	✓	×	✓	×
This Work	PDS	EEG + EMG, FPGA	✓	✓	✓	✓

Legend:
Acc: Accelerometers; FS: Foot switch; GA: Gait Analysis; Gyro: gyroscope; n.d.: not defined in the reference; PDS: Parkinson's disease stratification; RL-S: Suitable for a real-life scenario; RT: Real-time data processing

B. Theoretical Background

During voluntary movements, activation of proper muscles sequence is preceded by a cerebral preparation process that usually starts about 1s before muscle contraction and is accompanied by EEG potentials, called "Movement Related Potentials" (MRPs), which reveals the intentionality of movement [15]. In our work, we focused on three MRPs, i.e.

the Bereitschafts potential (BP), the μ rhythm, and the β rhythm. The BP is a slow positive component that increases progressively in amplitude starting from 1s before the movement and peaking about 100-200ms before the onset of movement. Its frequency band ranges between 2 and 5Hz. The signal has a 10μVmaximum amplitude [16]. The μ-rhythm occupies a frequency band between 9 and 11Hz and can occur up to 1s before the movement activation. Performing a motor action suppresses this rhythm [17]. The β-rhythm has a frequency band ranging from 12.5Hz to 30Hz. This pre-motor cortex rhythm is responsible for muscle contractions in isotonic movements [18]. Typically, MRPs are clearly visible in the brain hemisphere contralateral to the moving limb. A parallel deep knowledge of motor and cortical implications allows the objective investigation of cardinal features of the Parkinson's disease, according to the UPDRS scale [4]. This is possible, assuming that any involuntary movement is linked to muscle activation (EMG) without a phase motor ideation (EEG). This cortico-muscular approach defines the postural instability and returns a complete gait characterization. This is thanks to the deep differences in the walking pattern between PD patients and healthy subjects: PD subjects walk slowly, performing short shuffling steps and exhibit freezing episodes [1-4].

C. The Novel Cyber Physical System for Remote Gait Analysis

The CPS, outlined in Figure 1, is made up by: 8 wireless surface EMG and 8 EEG smart electrodes of the standard 32-channel electroencephalographic wireless headset.
The considered EEG electrodes are: T3, T4, C3, C4, CZ, P3, P4, according to the international 10-20 system [19, 20]. The O2 electrode is used for noise suppression.
As shown in Figure 2, the EMG electrodes are placed on Rectus and Biceps Femoralis, Gastrocnemius and Tibialis of both legs [22 - 25]. Both the EEG and the EMG signals are sampled at 500Hz, while the EMG has a 16bit resolution, the EEG are shown with 24bit of resolution [25]. Electrode signals are transmitted via Bluetooth to a dedicated gateway and processed in real-time by using an FPGA [23].
The workflow of the CPS can be summarized as follows. EEG and EMG data are analyzed at the same time by two parallel processing branches.
The EEG processing branch performs the time-frequency analysis on the EEG data acquired in the 500ms before the movement. Any limb muscle activation is detected by the EMG electrodes that trigger the EEG analysis. For the computation, we evaluate the MRPs and, in particular, the peak of the BP, the μ and β rhythm. The MRPs detection is based on thresholds definition and learning. In this way, our approach aims to realize a "truth machine of the involuntary movements" [25] to detect and quantify the cortical activity leading to a detected movement.
In parallel, the EMG processing aims to the instability detection by calculating a set of indexes quantifying both single muscles activity (contraction and relaxation times, step duty cycle - SDC) both behavior of agonist-antagonist muscles (agonist-antagonist muscle co-contraction time, number of co-contractions per second, named Haste Rate - HR).
By a dynamic threshold approach, each EMG signal is immediately converted in real time in a 1-bit signal (called in the following trigger), which is high only when the muscle is contracted.
The detected EMG contraction defines the acquisition trigger for the EEG. When the muscle activation edge occurs and all the MRPs overcome the thresholds (thus no critical situation is detected), the system extracts the Muscle Indexes (MI).
Although muscle tone and walk pattern are subjective parameters, in-vivo tests and literature references [19-21, 35] demonstrate that the co-contraction, can be an objective index for unbalance detection during the gait.
Basing on both experimental [20] and literature references [19, 35], the CPS interprets a co-contraction time (tcc) smaller than 400ms (lower threshold) as the indication of a normal pattern. In case of tcc exceeding 500ms (higher threshold), the system reports the presence of a significant instability. Finally, the range between 400ms and 500ms is used as a 'safety margin': when tcc is in this range, the algorithm takes into account the presence of a possible unbalance but this occurrence is not considered as a critical one. The co-contraction muscular indexes, together with the MRPs presence/absence, allow defining postural stability or involuntary movement onset.
On the other hand, the single muscle parameters (activation and relaxation time) contribute to the assessment of the bradykinesia (evaluating the slowness through the step duration) or abnormal unilateral muscular hyperactivity, in which the patient tends to incline the trunk on a particular side
In addition, they allow to uniquely assess motor fluctuations due to wrong treatment, by using a set of muscle activation/relax timers. Specifically, the system also calculates the step duty cycle, SDC, defined as:

$$\mathbf{SDC}(\%) = \frac{\mathbf{t_{con}}}{\mathbf{t_{con}+t_{rel}}} \cdot \mathbf{100} \qquad (1)$$

where t_{con} and t_{rel} are contraction and relaxation time on each muscle, respectively. Figure 3 summarizes all the MI definitions. In particular, Figure 3.a shows two trigger signals generated by the Left Rectus and the Biceps Femoralis. Figure 3.b shows the co-contraction and Figure 3.c displays the MRP spectral power levels referring to the first muscle activation and compare each of them to the correspondent fixed thresholds. When the CPS detects critical situation from either the EEG (critical motor-cortex involvements) or the EMG (abnormal co-contractions) processing branches, it provides an alert flag (Feedback in Fig.1) to the physician. The flag could be used to deliver either an external alarm or local feedback to the patient muscle (electrical stimulation for muscle activation) during the gait protocol or postural adjustment [4].

D. The Algorithm

The CPS is entrusted to the Altera Cyclone V SE 5CSEMA5F31C6N FPGA. The EMG and EEG signals are analyzed in parallel by two different computing paths in the FPGA.
In order to extract from the EMG signals the information about muscles activation/deactivation, the platform implements an

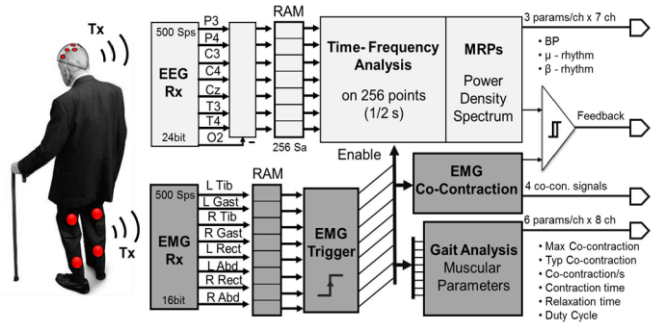

Fig 1. Cyber-physical system top-level architecture. EEG and EMG signals are wirelessly collected by a central unit, which includes an implementation of the proposed architecture. The architecture is here implemented on a FPGA.

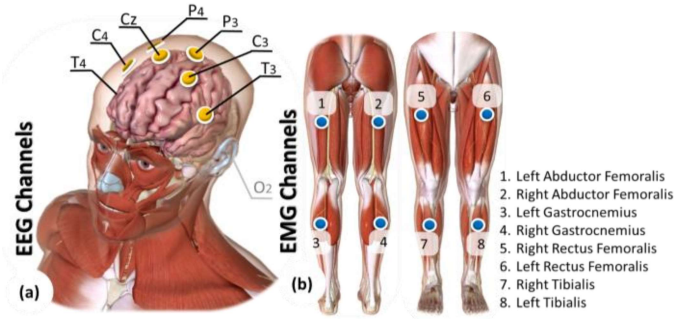

Fig. 2. (a) EEG and (b) EMG electrodes setting.

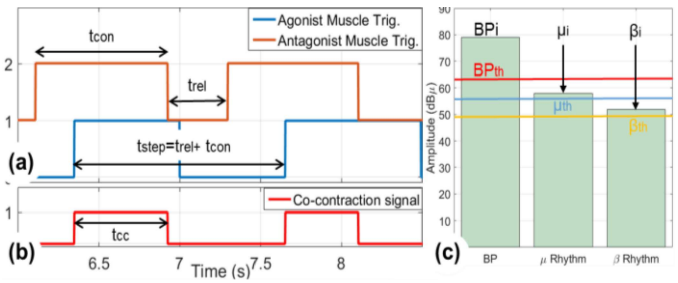

Fig. 3. Gait analysis parameters extraction. (a) agonist-antagonist muscle triggers. (b) the co-contraction signal obtained by the overlapping time of the triggers in (a). (c) Power spectrum of the MRP. A threshold level for MRPs on each step is outlined.

algorithm aiming to generate a 1-bit signal per EMG signal (EMG trigger) recorded [19 - 26].

Nevertheless, since the EMG is a signal with zero-mean and highly variable amplitude, a single threshold comparator approach cannot operate correctly. Movement artifacts and electrical noise can also affect it. Furthermore, even after an appropriate setting of the threshold, practical issues arise, such as the reduction of muscle tone during the medical evaluation, which could invalidate the diagnosis. Aiming to overcome the limits of a single threshold approach, the CPS exploits a procedure for a dynamic threshold extraction, starting from the raw data.

In the following, the procedure for the adaptive movement detection is detailed, considering, for clarity, a single EMG channel. The collected EMG signal is rectified, squared and stored in an shift-register. The shift-register stores 16-bits M words (in this work M = 512, i.e. 1s of the acquisition time). By averaging the samples in the register, the power of the signal (in the M-samples window) can be extracted. The computed power is named Global Power (GP) in this work and it is used as a temporary threshold.

A second average is calculated on the last N samples (with N<M) of the register (in this work N = 128, i.e. 250ms of the acquisition time). This second power level is called Local Power (LP). As soon as a new EMG sample arrives is received, both GP and LP are refreshed and the LP is compared to the GP: the dynamic movement detection consist of a 1-bit signal generated only when LP > GP.

Since the threshold is cyclically updated, the algorithm follows the trend of the muscular tone, continuing to work properly, even in case of supervening fatigue. The optimization in the trigger generation is based on the optimal choice of N and M. Specifically, when N is increased, a more reliable LP is extracted but - in spite of this benefit - the trigger activation is delayed. Aiming to avoid the random behavior of the trigger when the subject is at rest but standing, the LP undergoes a second threshold verification: the LP needs to overcome - in addition to the GP - a baseline, which is customized on the individual, after a period of learning [26].

The real-time signal processing of the EEG signals is presented in the following (only one EEG channel is presented for clarity). EEG are continuously stored in a 256 24-bit words shift-register (~500ms data).

As soon as the rising edge of the contralateral EMG occurs, a Fast Fourier Transform (FFT) is computed on the stored EEG. It should be stressed that the FFT is performed on 500ms before the muscle activation, in order to quantify the pre-motor potentials. The FFT output data are processed to extract the power levels in the proper MRPs bands. Subsequently, the computed output power levels, dynamically calculated as soon as a new muscle contraction is detected, are compared to static thresholds (one for each frequency band of BP_{th}, μ_{th}, and β_{th}) in order to evaluate the voluntariness of each EMG contraction. MRPs thresholds are subjectively calibrated basing on a stage of machine learning. In the calibration stage, the subjects were asked to stand, in the rest position, for about 1 minute without performing any movement and the MRP baseline is evaluated.

The movement is considered intentional and properly elaborated by the brain, only when MPR power levels are greater than the learned thresholds. All the under-threshold situations are considered as a mismatch between the movement performed and its brain processing (possible involuntary movement). Typically, MRPs are more visible in contralateral hemisphere with respect to the limb involved in the movement. These potentials are elicited into motor cortex area, i.e.: central and early parietal brain zone, with high relevance on the midline electrodes (C_3, C_z, C_4 - International 10-20 system [19, 20]) that typically refer to leg and foot movements [15].

Figure 4 summarizes the steps of the algorithm operation. First, EMG raw data are acquired in real-time (in Figure 4.a One channel out of 8 is shown for clarity). The red semi-transparency area represents the samples (NSa) that are considered for computing the LP; similarly, the yellow area represents the samples (MSa) used for the GP extraction. The EMG signal in Figure 4.a is processed in order to generate a Trigger (in Figure 4.b). The Trigger returns a high level when the local power (LP in Figure 4.b) is greater than the global one (GP in Figure 4.b). When the trigger rising edge occurs (red arrow in Figure 4.b), the EEG channels from the contra-lateral motor cortex hemisphere are processed by time-frequency

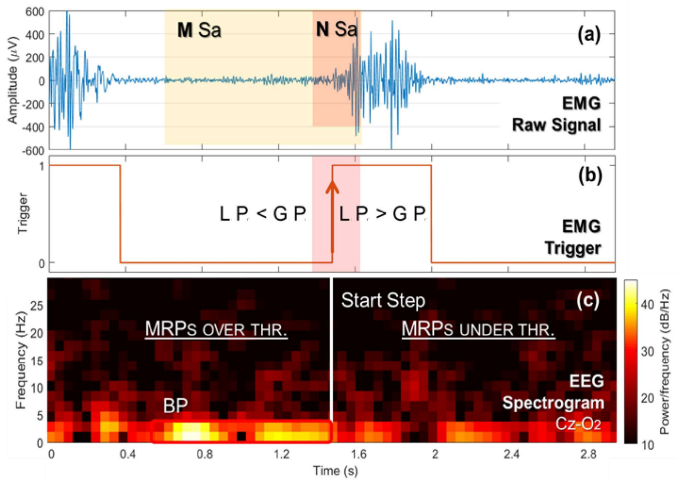

Fig. 4. Demonstrative algorithm workflow evaluated on a single step. (a) Raw EMG signal (blue - right Gastr.) and the windows for trigger generation (GP yellow and LP light red). (b) the associated Trigger signal (c) The FFT on the midline electrode Cz-O2 for the extraction of MRPs.

analysis. The time-frequency analysis adopted in this work is the Short Time Fourier Transform (STFT).
This method has been selected since it allows keeping the timing information (which is completely lost in a standard Fourier Transform) and, since it is computationally lighter than the Wavelet Transform, it is more suitable for real-time applications. Specifically, the EEG raw data is divided into slots of 500ms (i.e. 250 samples) by a sliding rectangular window. A first stage of noise reduction is performed by using a 'non-motor' EEG channel (O_2 in this work). Subsequently, the 'Fast Fourier Transform' (FFT) algorithm performs the spectral analysis of each EEG windowed signal. The spectral outcomes are labelled in the time domain by using the last sample analyzed in the window. Since the frequency resolution of the FFT is the ratio between the sampling frequency (f_{sEEG}=500 Sa/s) and the width of the window (250 Sa), the spectral resolution is 2Hz, which is enough for the band multiplexing. Instead, the time resolution is linked to the sliding step of the window, i.e. 50 samples or 100ms. Afterword, a 3D spectrogram is derived (Figure 4.c): time values are on the x-axis, the y-axis reports the frequency, while the absolute value of the signal FFT is reported using a different color scale. The contribute of the movement related potentials (EEGs), in the specific frequency bands, is expressed in the following in term of dBμ, which is by definition:

$$MRP|_{dB\mu} = 20 \cdot \log\left(\frac{MRP[V]}{1\mu V}\right) \qquad (2)$$

E. The FPGA Implementation

The above-described system has been physically prototyped by VHDL on an evaluation board provided by Terasic: DE1-SoC Rev.E, which embeds the Altera Cyclone V SE 5CSEMA5F31C6N FPGA. The prototyping set-up is shown in Fig. 5, where is possible to identify the Terasic board and the EEG/EMG signals readout and their canalization on the computing unit.
In our design, 16 bio-signals (8 EEG and 8 EMG channels) inputs and 57 outputs, have been used.

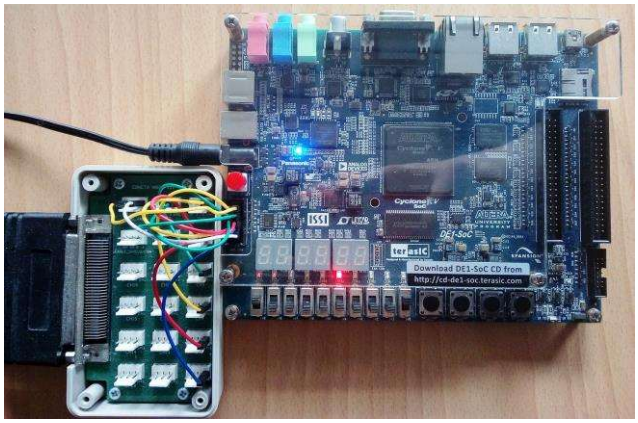

Fig. 4. System prototyping set-up: DE1-SoC evaluation board and bio-signals receiver

The inputs, coming from signal conditioning circuits [26-29], are serially canalized on 16 FPGA GPIO ports. Finally, they are filtered [30-33].
The 57 outputs, which are functionally distributed on the remaining available GPIO ports, consist of:

- 21 cortical parameters: BP, μ and β 1bit detection flags for each 7 motor-cortex channel. Thee flags rise to '1' if the MRP overcomes the baseline, otherwise '0'.
- 4 1bit co-contractions
- 4 co-contractions digitized with a dedicated counter in 11 bits. Thus, co-contraction time can assume a value between 0ms and 4094ms, considering 500Hz sampling rate. The extracted data have time resolution of 2ms.
- 8 contractions and 8 relaxation times extracted from a dedicated counter with 11 bits. As for the co-contraction, the contraction and relaxation times have 2ms of resolution and a full scale of about 4s.
- 8 7-bits duty cycles with 1% of sensitivity over the measured data.

The global signals are: the asynchronous Reset, the Enable SW which stops the processing; the 500Hz_CLK, sampling rate for both EMG and EEG. The adopted system clock is the 8MHz CLK (8.19209MHz), a clock signal derived by the on-chip Phase-Locked Loop (PLL) from the embedded 50MHz oscillator (50MHz_CLK).
The overall implementation is made up by 8 EMG and 7 EEG processing branches working in parallel on the FPGA.
The following section details the FPGA implementation of the algorithm.

F. The Computing Paths

EEG Branch. Figure 6 outlines a top-level workflow of a single EEG computing branch. The computation core of the considered branch is the FFT processor (256 points, 24 bit resolution), based on a *Radix-2 Butterfly Structure* (fixed point variable streaming FFT). The *Radix-2 Butterfly Structure* has been adopted for the Decimation-In Frequency because of its higher efficiency (it reduces the complex multiplications from N^2 to $N/2\log_2 N$, where N is the number of samples in the signal stream, 256 in our case) The EEG samples acquired are dynamically stored in a 256 24bit words RAM in FIFO configuration (EEG Ram) driven by the FFT Controller.

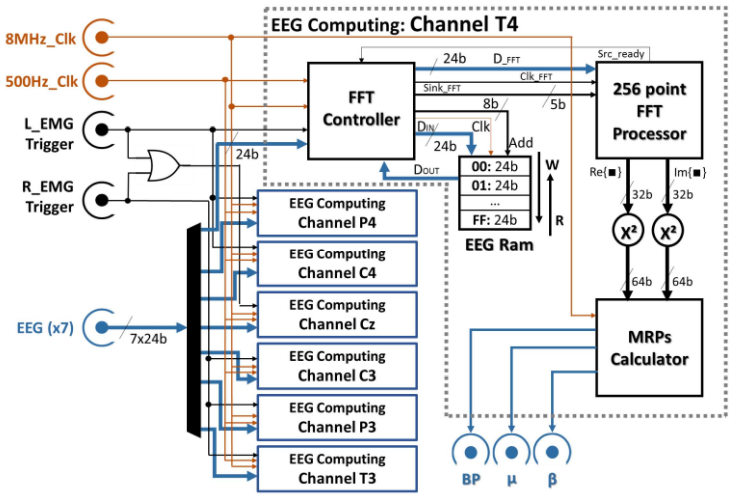

Fig. 6. Overview of the EEG branch.

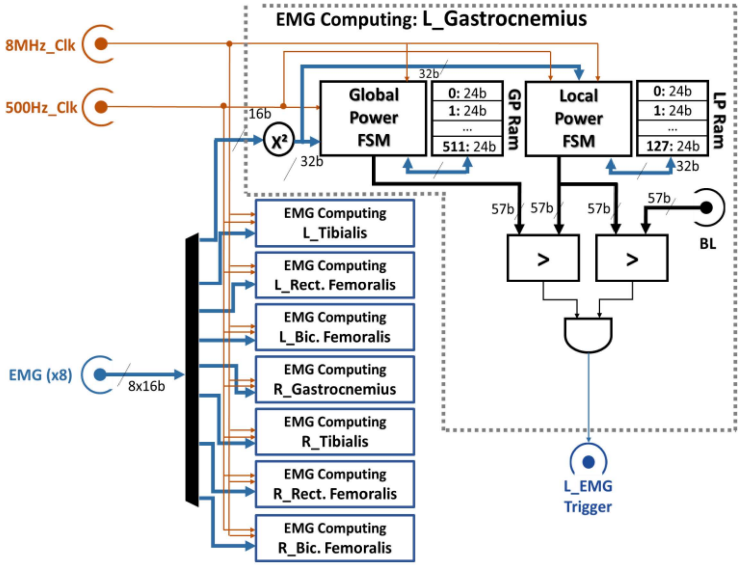

Fig. 7. Overview of the EMG branch.

As shown in Figure 6, the FFT Controller provides the data to be analyzed (D_FFT), the control signal for the FFT processor (Sink FFT) and a dedicated clock (Clk_FFT) @ 4MHz. The FSM in FFT Controller waits for the 500Hz_CLK rising edge, generating the RAM clock (Clk).

As shown Figure 6, if the L_EMG Trigger rises to '1', the RAM stored samples are transferred to the FFT processor by properly temporizing through a series of dedicated states (Sink). The FFT is done in less than 1ms.

Once the data are sent, the FSM waits for the FFT completion and finally passes the Real and Imaginary part to the MRP Calculator. The FSM for the MRP Calculator interprets the FFT output data, extracting the BP, μ and β powers, in natural units (BP, MU, BETA signals). Finally, BP, μ and β values are compared to static thresholds. The subjective thresholds are preloaded on the FPGA [22, 34].

EMG Branch. As shown in Figure 7, the EMG samples are squared (16bit to 32bit) and passed to two blocks named Global Power Finite State Machine (FSM) and Local Power one.

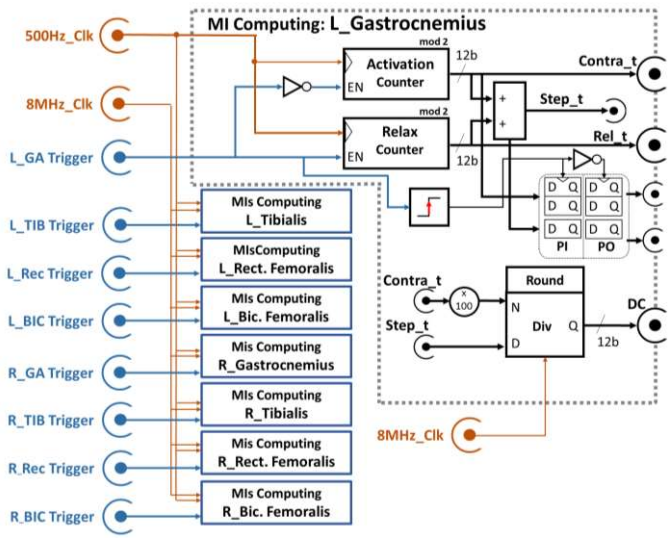

Fig. 8. Overview of the MIs branch.

The finite state machines calculate the dynamic threshold (GP) and the local power (LP). Basing on two block RAM (GP RAM 512 and LP RAM 128 in Figure 7), when a new EMG sample occurs, the last sample in RAM is extracted and returns in a FIFO-like functionality to proper FSM. The overall power within the window is refreshed by subtracting the previously RAM- extracted sample and by adding the new sample (Sum in follows). The FSMs overwrite the RAM word with the new data. Mathematically the FSM process can be expressed as:

$$\mathbf{Sum}: = \frac{\mathbf{M}\cdot\mathbf{S}-\mathbf{x}_n^2+\mathbf{x}_1^2}{\boldsymbol{M}} \quad (3)$$

where x_n^2 is the last squared sample extracted from the RAM block, x_1^2 is the new arrived sample, which is going to pick the first position in the RAM, M is the number of samples (512 for GP or 128 for LP) and S is defined in (4):

$$\mathbf{S} = \frac{\mathbf{1}}{\mathbf{M}} \cdot \sum_{\mathbf{i}=\mathbf{1}}^{\mathbf{M}} \mathbf{x}_\mathbf{i}^2 \quad (4)$$

where x_i^2 represents each sample arrived.

The 128bit based FSM differs from the 512bit based one, because in the LP Sum is divided by 128 (it consists of a 7bit right shift) while for the GA by 512 (9bit right shift).

At first, a three conditions comparator (>) compares the powers calculated by the two blocks (GP and LP) and then compares LP with the learned fixed threshold (BL). The comparator provides a 1bit EMG Trigger, used both in the EEG and Muscular Indexes (MI) computing branches.

MI Branch. Figure 8 schematically explains the process of indexes extraction from a single muscle. The branch operates serially with the generation of Trigger signal (EMG Branch output), and thus when the Trigger goes '1', the Activation Counter starts increasing its value by 1 bit, which corresponds to a 2ms increment (500Hz). Relax Counter operates in an analogous manner, but its increment is linked to the state '0' of the Trigger. At the end of the step, both the counters values are sent in output when the synchronization signal (Edge detector) goes high. A parallel bit sum (+) between realizes

Contra_t and Rel_t the step time. When the step is over (or another step starts), all the MI extracted until now are enabled to pass through a Parallel In- Parallel Out register (PIPO), which is piloted by the Edge detector signal.
When all the values are successfully transmitted downstream the PIPO, the counters are cleared. In this way, all the useful values (Activation Time, Step Time) are simultaneously present downstream from the PIPO for the entire next step time. This approach isolates the counting section, generating a static calculation section for the SDC. Here, the Contra_t is multiplied for $(100)_{10}$ and then divided by the entire step duration (Step_t). The quotient (Q) in output represents the integer value of the SDC (7bits). The remaining divider block is used for a rounding process.
In addition to single MI, also Agonist and Antagonist muscle Triggers are jointly evaluated, by using an AND gate, generating the co-contraction waveform. Similarly to Activation/Relax Counters operation, the co-contractions time are evaluated and returns its value when the step - in which the co-contraction is contained - ends. The Output Management block is used to refresh the output values on external device (e.g. set of display or website refresh) with an adequate timing.

III. Results

In the present section, a detailed report on the FPGA-based CPS performance is reported, focusing on the FPGA resources utilization, operation timing and power consumption. In addition, a section is dedicated to the in-vivo validation of the algorithm on 2 PD patients and 2 healthy subjects (control group).

A. FPGA Implementation Performances

In the acquisition frame, the CPS analyzes about 64kbps (500Sa/(s·ch) · 16bit/Sa · 8ch) from the EMG side and 84kbps (500Sa/(s·ch) · 24bit/Sa · 7ch) from the EEG. The system involves a total of 148kbps and provides outputs at 434bps. The CPS exploits 28894.7 adaptive logic modules out of 32070 available (90.1%), 419004 bits on memory block, where 4065280 are available (10.3%). In term of registers, the system uses the 74.8% (47996/64140). Table II summarizes the resources consumption by macro subsystems.
The EMG computing comprises the Global Power and Local Power FSMs, as well as RAMs block for the storage of the patterns. The EEG computing concerns, the FSMs for FFT controller/processor and MRPs calculation. The third entity (Single Muscle Indexes) represents the resources utilization for the extraction of Contra_t, Rel_t, SDC. The Coupled Muscles Indexes is related to the extrapolation of Co-Contraction time and HR for 4 agonist-antagonist couples. Other defines the surrounding circuitry.
By deeply analyzing the first two sub-systems, it is possible to quantify the contribution of each FSM in a single computing branch. The outcomes are shown in Figures 9 and 10.
Figure 9 shows the contribution in terms of resources utilization (ALMs, Registers and Memory) of the FSMs, in a single EMG branch. A single EMG branch consumes 268.8 ALMs, 188 Registers and 20480 bits of Memory blocks.

TABLE II. RESOURCES UTILIZATION BY SUB-SYSTEMS

SUB-SYSTEM	ALMs (TOT: 32070)	ALUTs	REGISTERS (TOT: 64140)	BLOCK MEMORY (BITS) (TOT : 4065280)
8 EMG Computing	1836.2 (5.7%)	3880	1432 (2.2%)	163840 (4.0%)
7 EEG Computing	23996 (74.8%)	40286	45227 (70.5%)	255164 (6.3%)
Single Muscle Indexes	2657.6 (8.3%)	5264	800 (1.3%)	0
Coupled Muscles Indexes	44.0 (0.14%)	48	120 (0.2%)	0
Others	360.9 (1.1%)	642	417(0.7%)	0 (0.0%)
Total	**28894.7 (90.1%)**	**50120**	**47996 (74.8%)**	**419004(10.3%)**

Fig. 9. Contribute in resources utilization of the FSMs that operates in a single EMG branches

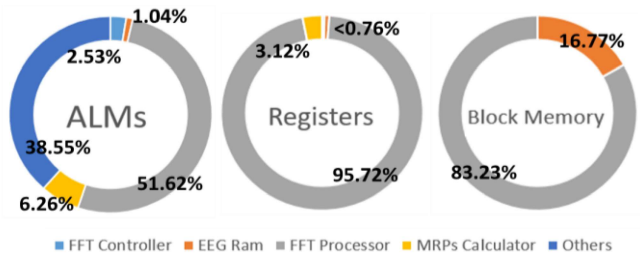

Fig. 10. Contribute in resources utilization of the FSMs that operates in a single EEG branches

Figure 10 reports the consumption (ALMs, Registers and Memory) of the FSMs in a single EEG branches. A single EEG branch consumes 4100.8 ALMs, 6994 Registers and 36632 bits of Memory blocks.
Figure 11 shows the Logic Array Block (LAB) utilization on the Altera Cyclone V FPGA, by using the Chip Planner Tool.
In particular, Figure 11.a reports the LAB utilization of the entire MI block (8 Single Muscle Indexes and 4 Coupled Muscles Indexes Extraction). The Figure 11.b shows the LAB utilization of the sub-system that implements the 8 EMG branches. The overall system is sketched in Figure 11.c, also comprising the 7 EEG blocks. In the Figure 11.d, it is shown by different colors, the increment in the LAB occupation, caused by the FFT blocks. Finally, the Figure 11.e represents a colormap of the wire utilization normalized to the available connection on the FPGA. The MI block involves the 2.9% of the total wire. For the EMG block, the routing utilization utility returns the 7.8%, while the 19% is dedicated to the EEG one, for a total of 29.7% of wire utilization.
In the timing requirements frame, the overall processing, from data collection up to FPGA output generation, requests about 57ms, matching the real-time constraints. In particular, the wireless recording system latencies are 1ms and 14ms, for multiplexing data digitalization and transmission, respectively. The EMG trigger is activated about 40ms after the actual

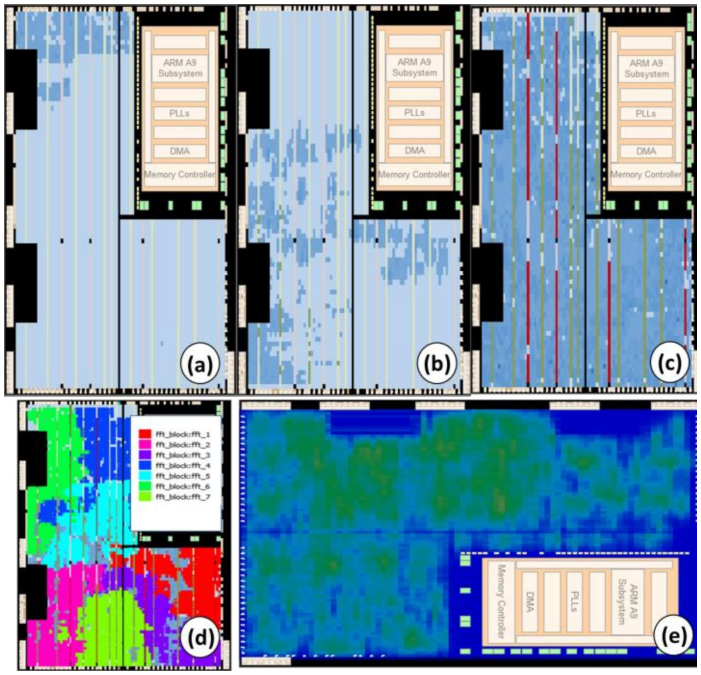

Fig. 11. LAB utilization of: (a) 8 MIs branches (b) 8 EMG branches (c) Overall system (d) FFT block locations (e) wire utilization colormap.

contraction [26] once the discrimination process of 10µs is performed. When enabled, the FFT runs in 0.13ms and the whole EEG processing, comprising the MRP calculation is completed in less than 1ms. The MI block operates, on average, each second but with a computing time of 0.2ms.

B. CPS Implementation Power Consumption

In a context of power consumption estimation, the here presented CPS, must be divided into two sub-systems: the sensors set and the computing unit (FPGA). Considering the first one, the wireless EMG sensors, operates with a power supply voltage of 4V (Lithium Battery of 28 x 20 x 12 mm), absorbing 40mW with a sampling rate of 2kHz and a transmission power (ARP) of 0.45mW@2.4MHz. In a continuous mode operation, the EMG nodes are able to send data for about 12 hours.

The EEG module uses an accumulator LIP 523450 3.7V has a rated power consumption on 500mW. A typical continuous acquisition reaches about 8 hours.

The PowerPlay Power Analyzer tool has been used to provide the power consumption values related to the computing unit (FPGA). All the data reported in the following have been obtained with a "*high*" power estimation confidence. The overall implementation consumes 519.57mW without heat sink with still air, of which 416.64mW is a core static thermal power dissipation. The P_{STATIC} is the thermal power dissipated on chip, independent of user clocks. It includes the leakage power from all FPGA functional blocks, except for I/O DC bias. The I/O management statically dissipated 8mW with a V_{DDIO}=2.5V. The adopted ADC (AD7928), operating with a serial clock of 20MHz and with a throughput rate of 500sps has a consumption of about 2.7mW, due to its operation in *full shutdown mode*.

The power dissipation caused by signal transitions (dynamically dissipated) is estimated as P_{DYN}=88.89mW, considering the two adopted clocks (`500Hz_Clk` and `8MHz_Clk`). P_{DYN} can be divided in: 14.4 mW for the I/O, 8.55mW for the register cells, 1.84mW for the combinational ones, the Memory 10 kB (M10K) blocks, dissipates 34.09mW, and finally, the PLL unit consumption is about 30mW.

C. *Study of the FPGA implementation in semicustom in 65nm CMOS technology*

The development of complex algorithms for domestic medical assistance systems is a challenging task, due to the high innovation rate and processing demands of applications in this field. The development is usually supported by a software, which provides an infrastructure (e.g., access to sensor data) that simulates and evaluates the algorithms. One problem, especially with computationally intensive algorithms, is the slow simulation speed. In this paper, we have presented a prototyping environment that connects a software development framework with a FPGA-based hardware platform. This allows implementing computationally intensive tasks in hardware. The proposed rapid prototyping system not only reduces the simulation time, thereby allowing the software designer to evaluate algorithmic parameters with quicker feedback, but also allows verifying and evaluating hardware modules for rapid prototyping. The degree of benefit can grow if the platform becomes portable or even wearable. In this aim, the future perspective of the method here described, is its implementation on an ad hoc ASIC design that can be easily embedded in a belt o in a swatch-type of holder. The benefits are: 1. area reduction and then portability, 2. power reduction, 3. Even faster performance evaluation and 4. better wireless communication. About the area, accordingly to a large set of benchmark circuits, largely detailed by Wong et al. in their work [37], a reliable area occupation estimation, for a semicustom CMOS 65nm implementation, can be made. In this aim, the equivalence between the implemented "building blocks" is necessary. Following the guidelines in [37], it is possible to describe our design as constituted by 46223 ALUTs, 228 M10k (10kb memory) and 87 complete DSP blocks. The tile areas of the above-listed blocks are respectively: 0.0011mm², 0.0635mm² and 0.2623mm². Considering the 65nm CMOS technology for the ASIC implementation, the area occupancy of the FPGA design, is about 70 mm² (considering as example, an off-the-shelf commercial device, in the same technology), as shown in Fig.11. As explained in [37], a rule of thumb to obtain a worst-case estimation of an equivalent 65nm semicustom CMOS circuit is to divide the area occupation for 27. In this way, but considering an additional optimization the here presented architecture, can potentially be compacted in less than 2 mm² die. The power can be estimated in a conservative mode as 100µW at 1.2V of supply (the max value in 65nm LP-CMOS technology) with a frequency of 300MHz [38]. The power consumption is reduced of almost three order of magnitude respect the ALTERA platform implementation, here described. The better communication is obviously given by the fixed distance between the transmitter (EEG/EMG) and the receiver (ASIC placed on the user belt).

D. *In-Vivo Testing and Validation*

The in-vivo testing and validation has been performed on a dataset of 2 patients affected by Parkinson disease (subject 1: age 61, male, body height 1.60m and body weight 58kg;subject 2: age 65, male, body height 1.73m and body weight 67kg) and 2 healthy subjects (subject 1: age 26, male, body height 1.77m and body weight 86kg; subject 2: age 25, male, body height 1.80m and body weight 80kg). To validate the proposed CPS, we used the following two standardized clinical protocols derived from the UPDRS guidelines [4]:

- 10-meter walk: Subjects walk for 10m distance. Subjects are asked to adopt a comfortable walking speed. The 10-meter walk is repeated for 10 times [4]. The test is prescribed by the sections: III.10 "March", III.11 "Freezing", III.13 "Postural Assessment", III.14 "Bradykinesia" and indirectly in motor complications section (UPDRS-IV) as IV.1 "Dyskinesia time" , IV.3 " Motor Fluctuations"
- Pull Test. The test evaluates the response to a sudden body displacement, induced by a rapid and vigorous traction on the shoulders while the patient is in an upright position. This test is prescribed by the section III.12 under the caption "Postural Stability" [4].

Specialized medical staff have supervised these tests which are prescribed by the UPDRS III and IV Parts [4]. The in-vivo testing was carried out in accordance with the recommendations of the ethics committee of the 'Azienda Ospedaliera Policlinico di Bari', Italy, with written informed consent from all subjects. All subjects gave written informed consent in accordance with the Declaration of Helsinki. The protocol was approved by the above-mentioned ethics committee. The CPS has been tested for three different applications: PD vs. Controls, Drug Treatment Evaluation and Involuntary Movements detection.
The experimental results have been reported in the following sub-paragraphs.

E. *PD vs. Control Group (PD Stratification)*

A systematic comparison between the PD extracted parameters and healthy subjects is provided in order to highlight the system suitability in disease recognition and stratification. The subjects (n. 2 PD subjects and n.2 Controls) are asked to perform the 10 meter walk protocol [4]. The results are presented in Table III, reporting the maximum and typical co-contraction time, the HR and the single muscle activation/relax time and SDC during a single step. Table III shows separately the parameters for PD (red background in Table II) and healthy subjects (blue background in Table III). All the indexes are expressed as mean±std. Also, the maximum co-contraction values are in the same form, since each one is referred to 2 subjects for each category. The results quantify the differences between PD subjects and healthy controls during gait:

- The maximum co-contraction time is higher in PD. The maximum co-contraction time detected for all muscles of the PD subjects is higher compared with the healthy subjects (e.g. on L. Rect-L. Bic. in PD subjects is 756ms and in healthy ones is 548ms).
- Co-contraction times during gait are higher in PD subjects than in healthy ones. Indeed, typical co-contraction time values show an increase of 18ms, on average, on the left side pairs, and an increment of 105ms on the right side between PD subjects and healthy ones. A great increment has been recorded on the right leg with +120ms on R.Gast and the coupled R. Tib; similarly, the couple R. Bic – R. Rect returns an increment of +90ms. The incidence on the right leg can be attributed to the patient's body flexion in that direction during his normal stationary state due to the Parkinson disease effect.
- Co-contractions are more frequent in PD. The average haste rates for PD subjects and healthy ones are 1.17 co-contractions/s and 0.44 co-contractions/s – respectively.
- The PD shows muscular hyperactivity during gait. On single muscle and on average, PD and healthy subjects show contraction time during the 48.56% and the 33.62% respectively of the step time width.

The difference in the walking patterns is also evident observing the diagram presented in Figure 12. The co-contractions are monitored on the Left Gastrocnemius and Tibialis muscles, while BP is evaluated on EEG channels from the right brain motor area. The areas in semi transparency (red for PD patients and blue for Control group) are delimited by a confidence interval of 67% of the evaluated (BP, tcc). The figure is derived considering a single 10-meter walk of a PD subject and a healthy individual due to the presence of exhaustive values for the comparison in Table III.
The analysis shows that both subjects provide comparable results concerning MRPs, while the co-contractions are clearly

TABLE III. MUSCULAR INDEXES EXTRACTED BY THE CPS IN PD VS. CONTROLS – PD: RED, CONTROLS: BLUE

	L REC	L BIC	R TIB	R GAS	L TIB	L GAS	R REC	R BIC
Coco Max (ms)	756±28		630±32		446±30		640±42	
	548±100		364±74		270±26		542±64	
Coco Typ (ms)	266±88		260±90		128±72		336±186	
	268±44		140±86		100±42		246±28	
HR (Cocon./s)	1.53±0.06		1.1±0.09		1.1±0.20		1±0.16	
	0.68±0.05		0.25±0.12		0.25±0.08		0.59±0.05	
Contra time (ms)	482 ±138	434 ±198	554 ±260	386 ±72	386 ±150	382 ±270	528 ±232	420 ±282
	353 ±128	509 ±198	574 ±208	382 ±170	560 ±254	444 ±110	328 ±142	494 ±182
Relax time (ms)	338 ±204	382 ±156	362 ±132	596 ±138	632 ±298	572 ±206	336 ±174	536 ±88
	982 ±498	788 ±361	632 ±282	868 ±392	950 ±266	980 ±230	982 ±438	812 ±368
SDC (%)	58±6	53±4	60±6	40±3	38±10	40±8	61±6	44±8
	26±3	39±5	48±6	31±2	37±7	31±5	25±3	38±8

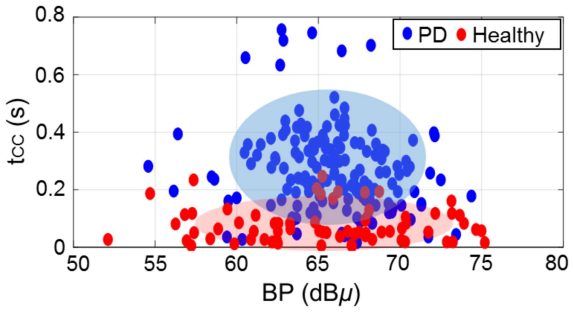

Fig. 12. BP vs co-contraction time for both PD (blue) and healthy subjects. The analysis outlines the different distribution of co-contraction times during gait.

more frequent and reach values much higher in the PD subjects than in the healthy ones. During the 10-meter walk, no significant differences on MRPs were found.
In Figure 12, it is possible to observe a slight broadening in the range of BP occurrence in healthy subjects.

These brain rhythms tend to focus with high probability at fixed values. The BP ranges from 58-65 dBμ, μ-rhythm from 51-55 dBμ and β-rhythm sweeps between 41-44 dBμ, for both subjects.

F. Drug Treatment Evaluation

This section is dedicated to the assessment of the CPS responses in term of cortico-muscular implications before and two hours after Levodopa administration. In this framework, PD subjects were asked to perform a natural and fluid walk, with comfortable speed in a straight path of 10m for 10 times (5 before and 5 after the treatment) within a total time range of 120 min, after the Levodopa administration. The results summarized in Table IV quantify the muscular implications of the drug treatment.
The parameters here reported and discussed are obtained considering the average on first 5 walks as "Before drug treatment" status (green background in Table IV), and the 5 final walks as "After drug treatment" status (red background in Table IV).

TABLE IV. MUSCULAR INDEXES EXTRACTED BY THE CPS IN DRUG TREATMENT EVALUATION – BEFORE AND AFTER TREATMENT.

	L REC	L BIC	R TIB	R GAS	L TIB	L GAS	R REC	R BIC
Coco Max (ms)	496		566		464		840	
	418		396		516		628	
Coco Typ (ms)	312±88		221±90		176±72		334±186	
	282.5±90		170±60		272±150		256±150	
HR (Cocon./s)	1.04±0.2		1,26±0.16		1,58±0.10		1,92±0.08	
	1.04±0.08		1.04±0.02		1.1±0.12		1.02±0.24	
Contra time (ms)	440±130	680±110	616±300	518±172	606±190	502±270	478±232	770±282
	444 ±108	568 ±130	613 ±228	470 ±272	650 ±130	552 ±250	446 ±200	614 ±130
Relax time (ms)	558 ±204	708 ±422	570 ±94	494 ±216	716 ±390	512 ±206	588 ±70	222 ±120
	642 ±136	372 ±222	296 ±122	466 ±108	404 ±144	416 ±300	540 ±88	414 ±266
SDC (%)	44±6	49±4	52±2	50±8	46±4	50±2	55±4	78±2
	41±2	60±3	67±4	50±7	62±3	57±5	45±5	60±7

TABLE V. MRPS EXTRACTED BY THE CPS IN DRUG TREATMENT EVALUATION – BEFORE AND AFTER TREATMENT.

		T3	P3	C3	CZ	C4	P4	T4
MRPs	BP(dBμ)	67.8±8.5	63.8±6.7	62.3±6.7	65.6±13	65.1±7.4	63.8±13	66.2±12
		60.7±6.3	62.3±5.6	62.7±5.4	62.4±5.1	60.9±5.9	62.4±5.2	62.9±5.7
	μ (dBμ)	49.2±2.3	50.1±2.9	49.0±2.4	47.9±9.1	47.0±9.0	52.3±9.5	49.0±9.0
		48.5±2.3	48.9±2.9	48.6±2.7	48.3±2.7	46.6±3.0	49.6±2.7	48.3±3.0
	β (dBμ)	40.1±3.3	41.0±2.8	39.6±2.3	39.6±7.5	40.1±7.2	45.0±4.3	40.8±2.8
		39.31±2	8.9±2.7	37.8±3.2	36.6±3.3	36.1±3.3	41.4±2.2	37.4±3.2

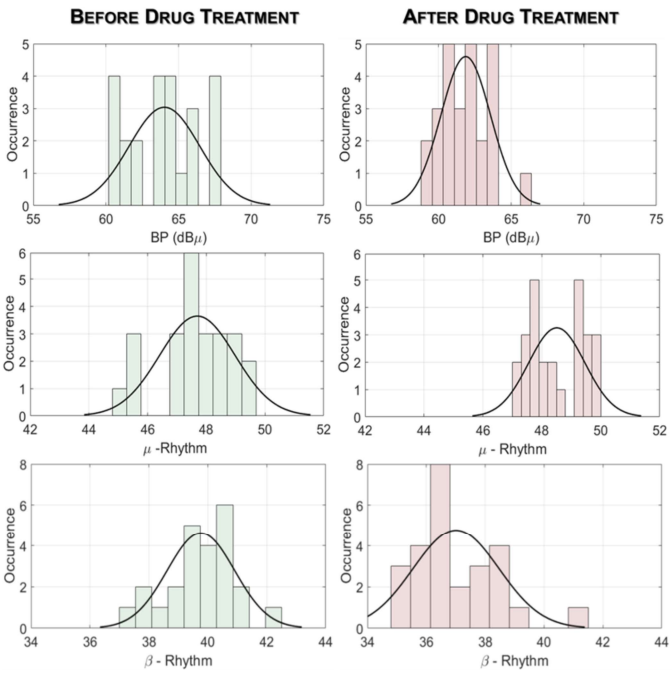

Fig. 13. The MRPs modulation evaluated on midline electrode Cz before (green) and after (red) the drug treatment.

The results contained in Table IV show that:

i. Before Levodopa administration PD subject had a maximum co-contraction time is of 840ms on R. Rect-R. Bic; while after the drug absorption, it reaches 628ms. The maximum co-contraction time is reduced of 23.6% after the treatment.
ii. The co-contractions show a decrease of 53ms (average value on all the four muscles couples), with a good improvement on the right leg (Δt=-51ms on R.Gast-R. Tib and Δt=-78ms on R. Bic – R. Rect). A postural recovery is induced by the Levodopa benefits.
iii. After Levodopa administration, the HR is reduced, on average, of 23.3%. PD subject exhibits 1.92 co-contractions/s and 1.02 co-contractions/s respectively before and after the treatment. Co-contractions are, on average, less frequent in PD patients after 120min from the treatment onset.
iv. The activation time on single muscle is reduced, on average, of 5.4% (576ms→544ms), similarly the relaxation is reduced of 18.8% (546ms→443ms). This behavior is linked to the loss of the slowness status. Indeed, step time after Levodopa is reduced of 100ms, reaching the duration of 1.1s starting from 1.2s.
v. On single muscle, the duty cycles follow an opposite trend, showing an average increase of 2.25%. It represents an increase of the muscular activity during the gait.

Gait analysis returns differences on MRPs value, showing a reduction of intentionality in the phase of motor ideation, typical of recurring movements (e.g. walking or go upstairs). Table V and Figure 13 show the Levodopa brain modulation in terms of BP μ and β rhythm mean and standard deviation of the probability density functions.

The x-axis and y-axis in Figure 13 are shared in order to highlight the differences in MRPs when the Levodopa starts to act. The BP before the Levodopa treatment (BP black Gaussian bell in Figure 13) has a mean of 64.9 dBμ and standard deviation of 9.61 dBμ.
After the Levodopa, the BP reaches a mean of 62.1 dBμ and a standard deviation of 5.6 dBμ. A relative reduction of 4.3% (2.8dBμ) in BP is recorded.
The μ- rhythm records an absolute increment of 0.8dBμ, or relative one of 1.6% (48.4dBμ±6.3dBμ → 49.2dBμ±6.3dBμ). Similarly to BP, the β-rhythm moves from 40.9dBμ±4.3dBμ to 38.2dBμ±2.8dBμ with a relative decrease of the 6% (2.7dBμ).

G. Detection of changes in postural stability

The CPS ability in detecting changes in postural stability is evaluated by using the pull test protocol, as detailed in sec. 3.D. The normal response to avoid the fall is one/two quick backwards steps followed by one forward recovery step. Usually, during this pull test, the physician associates a score to the subject reaction. In our case, the proposed CPS, quantifies the instability of the subject and his intentionality in the performed movements by evaluating the MRPs. Table VI reports the Pull test results for both PD and control subjects, including the mean value of MRPs for both right and left EEG monitored electrodes (the value is an average on all the premotor interested channels of both the subject involved in the test). It is important to note that the values of MRPs increase in an alternating manner, depending on the limb used to bring the step. For instance, considering only the BP values column, the results show that: starting from the 1st backward step, if we

TABLE VI. MRPS AND CO-CONTRACTIONS REVEALED BY THE CPS DURING PULL TEST FOR BOTH PD AND CONTROL GROUPS.

	Step	BP (dBμ)		μ-Rhythm (dBμ)		β-Rhythm (dBμ)		Max Co-cont. (ms)
		R	L	R	L	R	L	
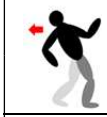	Inducted Fall	62.8	60	49.6	54	46.1	45.6	1060
		58.4	56.4	47.3	52.2	42.7	38.1	568
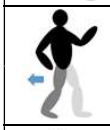	1st Back	65	62.4	54.5	54.7	46.3	44.3	598
		-	-	-	-	-	-	-
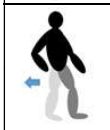	2nd Back	66	66.3	55.4	55.7	48.2	43.7	751
		-	-	-	-	-	-	-
	1st Recovery	69.3	66	55.8	57.9	44.8	47.9	98
		69.2	64.2	53.1	58.4	44.2	44.1	204
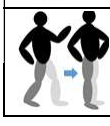	2nd Recovery	66	68.2	57.6	59.5	46.3	47	102
		-	-	-	-	-	-	-

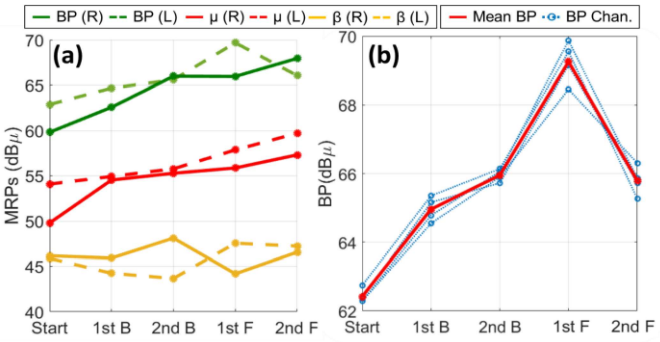

Fig. 14. (a) MRPs power levels behavior increment in the PD patient in order to recovery his stability. (b) BP average (red) extracted from each single channel response.

compare the BP extracted from left and right EEG channels, the larger values always alternated following the order: Right side BP (1st Back), Left side BP (2nd Back), Right side BP (1st Recovery), Left side BP (2nd Recovery). Both the sides increase their values.
Table VI also provides an indication of the maximum co-contraction value. The main results quantifying the differences between PD subjects and healthy controls are presented below:

i. PD subjects perform more settling steps. The EMG analysis demonstrates that, when the sudden unbalancing is externally induced, both the PD subjects reacted with four steps, two of whom were backwards. The other two steps were forward and completed the settling. The healthy subjects reacted to the test with one single settling step.

ii. PD co-contraction times are even longer in the pull test. PD subjects' co-contraction times increase, on average, of 98.75ms w.r.t. gait values, showing a situation of effective unbalancing. The healthy subjects' co-contraction values show no relevant change (increase of 11.75ms). The PD subjects' co-contraction maximum value was 1.06s and was recorded on right biceps-rectus Femoralis.

When a sudden unbalancing situation occurs, the PD subjects increase their initial value (that sweep between 59.9-62.8dBμ) of 6.5dBμ on right EEG channels and 6dBμ on left ones. The increase is progressive over the steps, clearly showing the recovery of voluntariness during the movements. The healthy subjects showed an initial range of 56.4-58.4dBμ and reached 64.2 dBμ (increase of 7.8 dBμ) and 69.2dBμ (increase of 7.8 dBμ) on left and right EEG channels, respectively.
The MRPs evolution of the PD subjects during a pull test is presented in Figure 14. The Figure 14.a clearly shows a rising trend for all the evaluated MRPs. The alternation between EEG left and right side in term of MRPs level is clearly present in BP and β-rhythms. Figure 14.b shows how the channels subjectively contribute to the average in Table VI. Figure 14 and Table VI show that the recorded MRPs values are comparable to the resting values under externally induced unbalance. However, in the recovery steps, the MRPs increase both on right (ΔBP = +11.9% ; Δμ =5.5% ; Δβ = + 11.1%) and left (ΔBP = +14.3% ; Δμ = +8.8% ; Δβ = +2.2%) EEG channels.

IV. Conclusion

In this work, a non-invasive wearable and wireless embedded cyber-physical system for PD monitoring has been implemented and tested on a programmable hardware. The CPS is made up by a wearable sensing system (8 EEG and 8 EMG wireless smart electrodes) and processing and synchronous data handling unit, based on an FPGA (Altera Cyclone V) as core, for real-time monitoring. The system calculates 57 different indexes, estimating the muscular implications during the movement and the motor cortex activity through the Movement Related Potentials. The implemented processing algorithm allows the system detecting critical situations during the gait, and thus to activate a corrective feedback action. In a future perspective of the system ASIC implementation, the choice of the implementation platform led on a programmable hardware, taking care to use only elementary components, without interactions/programming on the embedded processor (e.g. NiosII). The implemented architecture exploits the 90% of the ALMs, the 74% of the manageable registers and the 10.3% of the total memory, as well as the 29.7% wires utilization. In practical applications, the CPS is able to provide the outputs in about 57ms with a dynamically power dissipation of 89mW.
The processing system is self-adapting and the sensors non-invasive, can be wear by the patient without need of help or electrode positioning if EEG and EMG are respectively embedded in cap or sock. In such a way it is usable as assistive tool even in domestic environment and collect data over the day monitoring in remote of the drug impact in case of PD patients. The system has been in-vivo validated on a dataset of 4 patients. The experimental outcomes clearly show that the system can extract walking pattern differences between PD and healthy subjects, including agonist-antagonist co-contraction duration (i.e. Typical co-contraction of PD is, on average, 215ms higher than the same measure on a healthy subject). In the drug benefits/side effects evaluation application the CPS shows a reduction of 7% and 12% reduction in the typical and maximum co-contraction time, respectively, linked to the Levodopa administration. The system ability in fall recognition is proven with the pull test, in which all the monitored MRPs, increase during the voluntariness recovery.

References

[1] de Lau LM, Breteler MM (June 2006). "Epidemiology of Parkinson's disease". Lancet Neurol. 5 (6): 525–35. doi:10.1016/S1474-4422(06)70471-9.

[2] Larsen, T. A., P. A. LeWitt, and D. B. Calne. "Theoretical and practical issues in assessment of deficits and therapy in parkinsonism." Lisuride and other dopamine agonists. Raven, New York (1983): 363-373.

[3] R. L. Watts and A. S. Mandir,“ Quantitative methods of evaluating Parkinson’s disease,” in The Scientific Basis for the Treatment of Parkinson’s Disease, C. W. Olanow and A. N. Lieberman, Eds. Park Ridge: Parthenon, 1992, pp. 13–32.

[4] Vassar, S. D., Bordelon, Y. M., Hays, R. D., Diaz, N., Rausch, R., Mao, C., &Vickrey, B. G. Confirmatory factor analysis of the motor unified Parkinson’s disease rating scale. Parkinson’s Disease, 2012.

[5] De Venuto, D., Vincentelli, A.S. “Dr. Frankenstein's dream made possible: Implanted electronic devices” (2013) Proceedings -Design, Automation and Test in Europe, DATE, art. no. 6513757, pp. 1531-1536.

[6] M. Goffredo, R. D. Seely, J. N. Carter and M. S. Nixon, "Markerless view independent gait analysis with self-camera calibration," 2008 8th IEEE International Conference on Automatic Face & Gesture Recognition, Amsterdam, 2008, pp. 1-6. doi: 10.1109/AFGR.2008.4813366

[7] Terrier, Philippe, and Yves Schutz. "How useful is satellite positioning system (GPS) to track gait parameters? A review." Journal of neuroengineering and rehabilitation 2.1 (2005): 28.

[8] Klucken J, Barth J, Kugler P, Schlachetzki J, Henze T, Marxreiter F, et al. (2013) Unbiased and Mobile Gait Analysis Detects Motor Impairment in Parkinson's Disease. PLoS ONE 8(2): e56956. doi:10.1371/journal.pone.0056956

[9] Griffiths, R. I., et al. Automated assessment of bradykinesia and dyskinesia in Parkinson’s disease. J Parkinson’s Dis 2 (1): 47–55. doi: 10.3233. JPD-2012-11071, 2012.

[10] Han, J., et al. "Gait detection from three dimensional acceleration signals of ankles for the patients with Parkinson’s disease." Proceedings of the IEEE The International Special Topic Conference on Information Technology in Biomedicine, Ioannina, Epirus, Greece. Vol. 2628. 2006.

[11] Lubik, S., et al. "Gait analysis in patients with advanced Parkinson disease: different or additive effects on gait induced by levodopa and chronic STN stimulation." Journal of neural transmission 113.2 (2006): 163-173.

[12] Rodríguez-Martín D, Pérez-López C, Samà A, Cabestany J, Català A. A Wearable Inertial Measurement Unit for Long-Term Monitoring in the Dependency Care Area. Sensors. 2013 Oct 18 [cited 2017 Apr 4];13(10):14079–104.

[13] Rodríguez-Molinero, Alejandro, et al. "Validation of a portable device for mapping motor and gait disturbances in Parkinson’s disease." JMIR mHealth and uHealth 3.1 (2015).

[14] Tzallas, A. T., Tsipouras, M. G., Rigas, G., Tsalikakis, D. G., Karvounis, E. C., Chondrogiorgi, M., Psomadellis F., Cancela J., Pastorino M., Arredondo Waldmeyer M.T., Konitsiotis S. and Fotiadis, D. I.. PERFORM: A System for Monitoring, Assessment and Management of Patients with Parkinson’s Disease. Sensors, 14(11), 21329-21357, 2014

[15] De Tommaso, M., Vecchio, E., Ricci, K., Montemurno, A., De Venuto, D., Annese, V.F. “Combined EEG/EMG evaluation during a novel dual task paradigm for gait analysis.” (2015) Proceedings - 2015 6th IEEE International Workshop on Advances in Sensors and Interfaces, IWASI 2015, art. no. 7184949, pp. 181-186. DOI: 10.1109/IWASI.2015.7184949

[16] Kornhuber, Hans H., and Lüder Deecke. "Brain potential changes in voluntary and passive movements in humans: readiness potential and reafferent potentials." Pflügers Archiv-European Journal of Physiology 468.7 (2016): 1115-1124.

[17] Muthukumaraswamy, S. D. et al. "Mu- rhythm modulation during observation of an object-directed grasp". Brain Res Cogn Brain Res 19 (2): 195–201.2004.

[18] Zhang, Y; Chen, Y; Bressler, SL; Ding, M (2008). "Response preparation and inhibition: the role of the cortical sensorimotor beta rhythm". Neuroscience 156 (1): 238–46. doi:10.1016/j.neuroscience.2008.06.061. PMC 2684699.

[19] S. Bounyong et al., "Fall risk estimation based on co-contraction of lower limb during walking," 2016 IEEE International Conference on Consumer Electronics (ICCE), Las Vegas, NV, 2016, pp. 331-332. doi: 10.1109/ICCE.2016.7430634

[20] Annese, V.F., De Venuto, D. “Fall-risk assessment by combined movement related potentials and co-contraction index monitoring”. (2015) IEEE Biomedical Circuits and Systems Conference: Engineering for Healthy Minds and Able Bodies, BioCAS 2015 - Proceedings, art. no. 7348366. DOI: 10.1109/BioCAS.2015.7348366

[21] Annese, V.F., De Venuto, D. “Gait analysis for fall prediction using EMG triggered movement related potentials.” (2015) Proceedings - 2015 10th IEEE International Conference on Design and Technology of Integrated Systems in Nanoscale Era, DTIS 2015, art. no. 7127386. DOI: 10.1109/DTIS.2015.7127386

[22] Y. Lajoie et al. “Predicting falls within the elderly community: Comparison of postural sway, reaction time, the Berg balance scale and the Activities-specific Balance Confidence (ABC) scale for comparing fallers and non-fallers”, Arch. gerontology-geriatrics, 38.1:11-26, 2014.

[23] Annese, V.F., De Venuto, D. “FPGA based architecture for fall-risk assessment during gait monitoring by synchronous EEG/EMG.” (2015) Proceedings - 2015 6th IEEE International Workshop on Advances in Sensors and Interfaces, IWASI 2015, art. no. 7184953, pp. 116-121. DOI: 10.1109/IWASI.2015.7184953

[24] De Venuto, D., Annese, V.F., Ruta, M., Di Sciascio, E., Sangiovanni Vincentelli, A.L. “Designing a Cyber-Physical System for Fall Prevention by Cortico-Muscular Coupling Detection.” (2016) IEEE

Design and Test, 33 (3), art. no. 7273831, pp. 66-76. DOI: 10.1109/MDAT.2015.2480707
[25] Annese, V.F., De Venuto, D. "The truth machine of involuntary movement: FPGA based cortico-muscular analysis for fall prevention" (2016) 2015 IEEE International Symposium on Signal Processing and Information Technology, ISSPIT 2015, art. no. 7394398, pp. 553-558. DOI: 10.1109/ISSPIT.2015.7394398.
[26] V. F. Annese, M. Crepaldi, D. Demarchi and D. De Venuto, "A digital processor architecture for combined EEG/EMG falling risk prediction," 2016 Design, Automation & Test in Europe Conference & Exhibition (DATE), Dresden, 2016, pp. 714-719.
[27] De Venuto, D., Castro, D. T., Ponomarev, Y., Stikvoort, E. "Low power 12-bit SAR ADC for autonomous wireless sensors network interface," 2009 3rd International Workshop on Advances in sensors and Interfaces, Trani, 2009, pp. 115-120. doi: 10.1109/IWASI.2009.5184780
[28] De Venuto, D., Ohletz, M. J., and B. Ricco, "Testing of analogue circuits via (standard) digital gates" Proceedings International Symposium on Quality Electronic Design, 2002, pp. 112-119. doi: 10.1109/ISQED.2002.996709
[29] De Venuto, D., Stikvoort, E., Tio Castro, D., Ponomarev, Y. "Ultra low-power 12-bit SAR ADC for RFID applications" (2010) Proceedings - Design, Automation and Test in Europe, DATE, art. no. 5456968, pp. 1071-1075. DOI: 10.1109/DATE.2010.5456968
[30] Daniela De Venuto, David Tio Castro, Youri Ponomarev, Eduard Stikvoort, 0.8μW 12-bit SAR ADC sensors interface for RFID applications, Microelectronics Journal, Volume 41, Issue 11, 2010, Pages 746-751, ISSN 0026-2692, DOI: 10.1016/j.mejo.2010.06.019.
[31] De Venuto, D., Stikvoort, E. Low power high-resolution smart temperature sensor for autonomous multi-sensor system (2012) IEEE Sensors Journal, 12 (12), art. no. 6202316, pp. 3384-3391. DOI: 10.1109/JSEN.2012.2198915
[32] D. De Venuto, D. T. Castro, Y. Ponomarev and E. Stikvoort, "Low power 12-bit SAR ADC for autonomous wireless sensors network interface," 2009 3rd International Workshop on Advances in sensors and Interfaces, Trani, 2009, pp. 115-120 doi:10.1109/IWASI.2009.5184780
[33] D. De Venuto, M. D. Torre, C. Boero, S. Carrara and G. De Micheli, "A novel multi-working electrode potentiostat for electrochemical detection of metabolites," 2010 IEEE Sensors, Kona, HI, 2010, pp. 1572-1577. doi: 10.1109/ICSENS.2010.5690297
[34] D. De Venuto, M. J. Ohletz and B. Riccò, "Automatic repositioning technique for digital cell based window comparators and implementation within mixed-signal DfT schemes," Fourth International Symposium on Quality Electronic Design, 2003. Proceedings., 2003, pp. 431-437 doi:10.1109/ISQED.2003.1194771
[35] Fallah-Yakhdani, Hamid R., et al. "Determinants of co-contraction during walking before and after arthroplasty for knee osteoarthritis." Clinical Biomechanics 27.5 (2012): 485-494.
[36] Twelves Dominique, Perkins Kate S, Counsell Carl. Systematic review of incidence studies of Parkinson's disease. Mov Disord. 2003 Jan;18(1):19–31. doi: 10.1002/mds.10305.
[37] Wong, Henry, Vaughn Betz, and Jonathan Rose. "Comparing FPGA vs. custom CMOS and the impact on processor microarchitecture." Proceedings of the 19th ACM/SIGDA international symposium on Field programmable gate arrays. ACM, 2011.
[38] Meijer, Maurice, and José Pineda de Gyvez. "Technological boundaries of voltage and frequency scaling for power performance tuning." Adaptive Techniques for Dynamic Processor Optimization. Springer US, 2008. 25-47.

Daniela De Venuto is professor of Electronics at Politecnico di Bari, Italy. She leads the Design of Electronic Integrated System Laboratory (DEISLab). She initiated the bi-annual IEEE Advances in Sensors and Interfaces Workshop (IWASI), which successfully continues since 2005. Since 2010, she is an IEEE ISQED Fellow. She has been a visiting professor in several outstanding Universities and Research Centers in Europe and the U.S. Currently, she is collaborating with the Department of Electrical Engineering and Computer Science, University of California at Berkeley, Berkeley, CA, USA. She is the main investigator of several research projects founded by Ministry of the University and private companies, on design of conditioning electronics for sensors in healthcare applications. Her main scientific interests are on design of CMOS analog and mixed-signal IC, smart sensors and biosensor. Recently she is also involved in IC design for Brain Machine Interface (BMI).

Valerio Francesco Annese received the B.Eng. degree in electronic and telecommunication engineering and the M.Sc. (Magna cum laude) degree in electronics engineering from the 'Politecnico di Bari', Bari, Italy in 2014 and 2016 respectively. From 04/2014 to 11/2016 he was research assistant at the Design of Electronic Integrated System Laboratory (DEISLab) at the 'Politecnico di Bari' where his research topics included IC Design, FPGA programming and bio signals processing (i.e. EEG and EMG). Currently, he is working toward the Ph.D. degree in electronic and electrical engineering at the University of Glasgow (UK) with the Microsystem Technology group. His research fields include chip post-processing, nano-electronics, device fabrication, bio-electronics, surface functionalization, flexible electronics and drop on demand (DoD) inkjet printing. He is a member of the IEEE.

Giovanni Mezzina is a research assistant with the Politecnico di Bari, Italy, working in the Design of Electronics Integrated Systems Lab (November 2015 - onwards). He received the B.Eng. degree in electronic and telecommunication engineering in 2016. His research interests include acquisition and processing of the bio signals (EEG, EMG), and their use in brain computer interface, brain-control of mechatronic devices. He is also involved in the development of tools for the optimal design of switched power amplifier. He is a member of the IEEE.

Giovanni Defazio is professor of Neurology at the University of Bari, Italy since 2004. Since 2002 he has been the principal investigator in a number of research projects funded by the Italian Ministry of University and research (MURST), University of Bari, and national and international foundations. He is a member of "The Movement Disorders Society", the "Italian Society of Neurology (SIN)", the "Lega Italiana cotro la malattia di Parkinson e le Malattie Extrapiramidali (LIMPE)". From 2011 he is the President of the "Associazione Italiana disordioni del Movimento e Malattia di Parkinson". Currently, he is the author of more than 120 peer-rewieved articles published in international scientific journals, four chapters of neurological books, more than 200 contributes to national and international scientific meetings.